

Neodymium disilicate ceramic pigment synthesized by solid-state method with pre-grinding and mineralizer

Shanjun Ke^a, Yanmin Wang^{a,*}, Zhidong Pan^{a,b,*} and Heping Zeng^a

^aSouth China University of Technology, Guangzhou 510640, China

^bFoshan Oceano Ceramics Co. Ltd., Foshan 528138, China

A ceramic pigment of neodymium disilicate (i.e., $\text{Nd}_2\text{Si}_2\text{O}_7$) was synthesized *via* solid-state reaction with pre-grinding assistance and a mineralizer. The effects of pre-grinding and mineralizer (i.e., lithium chloride, boric acid and calcium fluoride) on the phase, microstructure and coloring properties of ceramic pigment were investigated by differential thermal analysis, X-ray diffraction, scanning electron microscopy and reflectance spectra in the visible range from 400 nm to 700 nm, respectively. The results show that the reaction temperature of $\text{Nd}_2\text{Si}_2\text{O}_7$ can be decreased by pre-grinding, and the temperature of forming sole $\text{Nd}_2\text{Si}_2\text{O}_7$ phase is further decreased by 200 °C when lithium chloride is used as a mineralizer. Boric acid as a mineralizer can lead to an uneven distribution of Nd and Si components. The sample synthesized with calcium fluoride as a mineralizer cannot obtain $\text{Nd}_2\text{Si}_2\text{O}_7$ phase. $\text{Nd}_2\text{Si}_2\text{O}_7$ can be synthesized effectively when lithium chloride is used as a mineralizer.

Key words: Neodymium disilicate, Ceramic pigment, Solid-phase reaction, Pre-grinding, Mineralizer.

Introduction

Ceramic pigments as a kind of decorative material are usually used to color glazes or ceramic bodies [1, 2]. In recent years, ultrafine and functional ceramic pigments have attracted extensive attentions [3-5]. The ultrafine pigments are typically applied to ceramic substrates by ink-jet printing [5]. Some ceramic pigments with a high near infrared reflectance can well serve as cool colorants [6, 7]. Also, our previous work [8, 9] reported that neodymium disilicate (i.e., $\text{Nd}_2\text{Si}_2\text{O}_7$) powder prepared by wet chemical synthesis methods, which can be used as a potential functional pigment with allochroic effect under various illuminants. In fact, solid-state reaction is a more promising and effective method for processing $\text{Nd}_2\text{Si}_2\text{O}_7$ pigment [10]. This method usually requires the application of high temperatures and/or prolonged processing time for calcination. It is thus important for the energy-saving and effective process to reduce the heat-treatment temperature and time in solid-state reaction. As is well known, the pretreatment of raw materials by ultrafine grinding can effectively reduce the formation temperature of reactant in subsequent calcination [11]. The refinement of the raw materials increases the contact surface area between the particles and accelerates the progress of the reaction. The energy from grinding can

cause a chemical reaction among the raw material particles [12, 13]. In addition, a mineralizer is usually used as a low-temperature flux to decrease the solid-state reaction temperature. Different types of mineralizer have different effects on the properties of synthetic materials due to differences in the melting point and high-temperature reaction of mineralizer. Chloride [14], fluoride [15] and boron-containing compound [16] are several common mineralizers with a low cost for ceramic industry. However, little work on the effect of mineralizer on the solid-state reaction synthesis of $\text{Nd}_2\text{Si}_2\text{O}_7$ pigment has been carried out so far. In this paper, $\text{Nd}_2\text{Si}_2\text{O}_7$ pigment was synthesized *via* solid-state reaction. The effects of pre-grinding and mineralizer (i.e., LiCl , H_3BO_3 and CaF_2) on the microstructure and coloring properties of $\text{Nd}_2\text{Si}_2\text{O}_7$ pigment were investigated.

Experimental

Neodymium oxide (Nd_2O_3 , 99.5 %, Ganzhou Ruihua Rare Earth Co., Ltd., China), silicon oxide (SiO_2 , AR, Sinopharm Chemical Reagent Co., Ltd., China), modified polyacrylate (Minchem Chemical, Co., Ltd., France), three kinds of mineralizers (i.e., LiCl , H_3BO_3 and NaF , Fuchen Chemical Reagents Factory, China) and deionized water (H_2O , Guangzhou Qianghui Bose Instrument Co., Ltd., China) were used as starting materials.

Nd_2O_3 and SiO_2 were mixed to obtain the stoichiometric composition of $\text{Nd}_2\text{Si}_2\text{O}_7$ with 5 wt.% of the modified polyacrylate as a grinding aid. The mixture with 40 wt.% deionized water was ground in a model WS-0.3 ceramic stirred bead mill (Sanxing

*Corresponding author:

Tel : +86 20 8711 4883

Fax: +86 20 87110273

E-mail: wangym@scut.edu.cn (Y.M. Wang),
panzd@scut.edu.cn (Z.D. Pan)

Feirong Machine Ltd., China) at 1995 rpm for 3 h. Zirconium oxide beads with the diameters of 0.3-0.5 mm were used as grinding media at a bead loading of 80 vol.%. The ground suspension was heated to 80 °C and kept at this temperature for 24 h. The dried materials with 5 wt.% mineralizer (i.e., LiCl, H₃BO₃ or CaF₂) was ground in an agate mortar and calcined at 900, 1000 and 1100 °C for 5 h, respectively. The calcined powders were subjected to wet-milling in a planetary mill with small zirconia balls for 1 h. The pigment powders were obtained after drying. The pigment was added into transparent frit glaze (chemical composition: 53.24 % SiO₂, 11.89 % Al₂O₃, 0.12 % Fe₂O₃, 0.01 % TiO₂, 12.20 % CaO, 4.58 % MgO, 10.36 % ZnO, 4.69 % K₂O and 2.91 % Na₂O) and coated on a ceramic tile. The coated ceramic tile was sintered at 1200 °C for 10 min.

The particle size distribution of the samples was determined by a model BT-9300S laser diffraction particle size analyzer (Bettersize Instruments Ltd., China). The thermal analysis of the prepared precursors was carried out by a simultaneous thermogravimeter and differential thermal analyzer (DTA, Netzsch Instruments Ltd., Germany), at a heating rate of 10 °C/min, in air, using α -Al₂O₃ as a reference. The crystalline phases of the powder were examined on a model PW-1710 X-ray diffractometer (XRD, Philips Co., Ltd., The Netherlands), using Cu K α radiation. The morphology of the powder samples was inspected by a model EVO-18 scanning electron microscope (SEM, Carl Zeiss AG, Germany). The optical absorption spectra of pigment powders were recorded by a mode Cary 5000 UV-vis-NIR diffuse reflectance spectroscopy, using a BaSO₄ integrating sphere.

Results and discussion

Fig. 1 shows the particle size distributions of the raw material mixtures without mineralizer unground and ground at 3 h, respectively. For the unground mixture, the median particle size is 2.76 μ m. At the grinding time of 3 h, the median particle size decreases to 0.34 μ m.

Fig. 2 shows the XRD patterns of the raw material mixtures unground and ground at 3 h. Clearly, the pattern of the unground mixture shows the presence of Nd₂O₃, SiO₂ and Nd(OH)₃. The phase of Nd(OH)₃ is due to the reaction result of Nd₂O₃ and water. This could be due to the adsorption of water on Nd₂O₃ at room temperature [17]. The hydration process is that Nd₂O₃ first changes to NdOOH and then to Nd(OH)₃. In addition, the diffraction intensities of SiO₂ and Nd(OH)₃ decrease when the grinding time is 3 h. It can be explained that the high-energy milling process affects the crystallinities of SiO₂ and Nd(OH)₃.

Fig. 3 shows the XRD patterns of the raw material mixtures without mineralizer unground and ground at 3

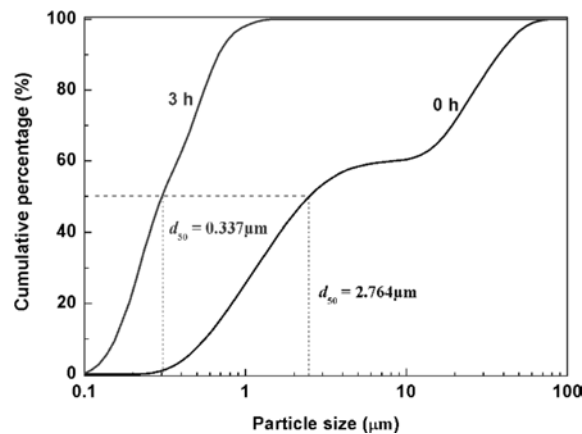


Fig. 1. The particle size distributions of raw material mixtures without mineralizer unground and ground at 3 h.

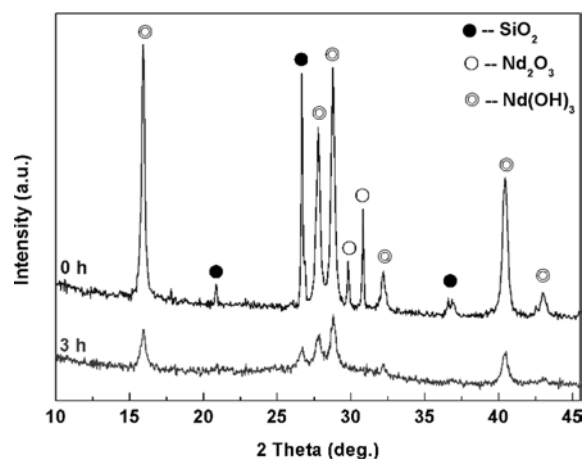


Fig. 2. The XRD patterns of raw material mixtures unground and ground at 3 h.

h and heat-treated at different temperatures. For the raw material mixtures unground and heat-treated at \leq 1100 °C, there are only two phases (i.e., Nd₂O₃ and SiO₂). For the unground mixture heat-treated at 1200 °C, Nd₄Si₃O₁₂ crystalline phase and a small amount of SiO₂ occur, but no Nd₂Si₂O₇ phase appears. After 3-h grinding, the phase is Nd₄Si₃O₁₂ for the mixture heat-treated at \leq 1000 °C. When the sintering temperature increases to 1100 °C, Nd₂Si₂O₇ becomes a sole crystalline phase. These results indicate that high-energy milling process can improve the reactivity of raw materials and decrease the reaction temperature of Nd₂Si₂O₇.

Fig. 4 shows the TG and DTA curves of the raw material mixtures unground and ground at 3 h. For the unground raw material mixture, there are three stages of weight loss on the TG curve. The first stage of weight loss (i.e., 8.84 %) is due to the dehydroxylation and burning out of organic compounds. Nagao et al. [18] also reported that Nd(OH)₃ can be changed to NdOOH at 200-400 °C. The second stage of weight loss (i.e., 2.3 %) corresponds to the further dehydroxylation. Zhu et al. [19] found that the decomposition temperature

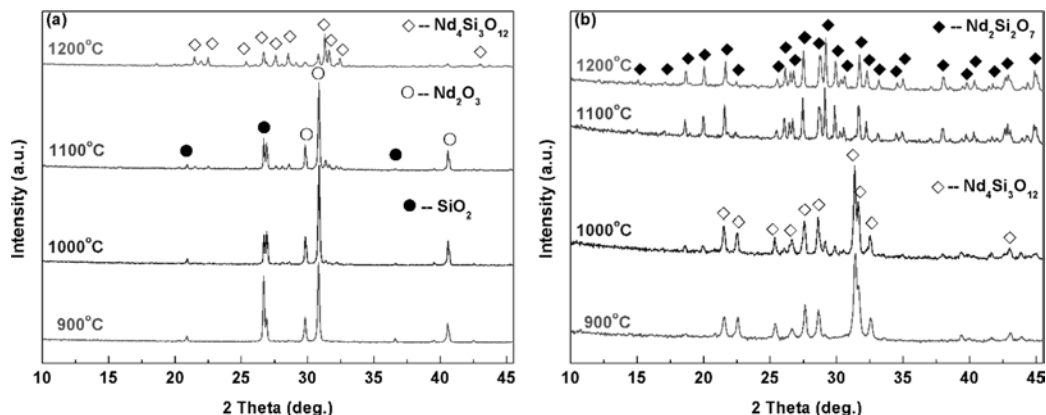


Fig. 3. The XRD patterns of the raw material mixtures without mineralizer unground (a) and ground at 3 h (b) and heat-treated at different temperatures.

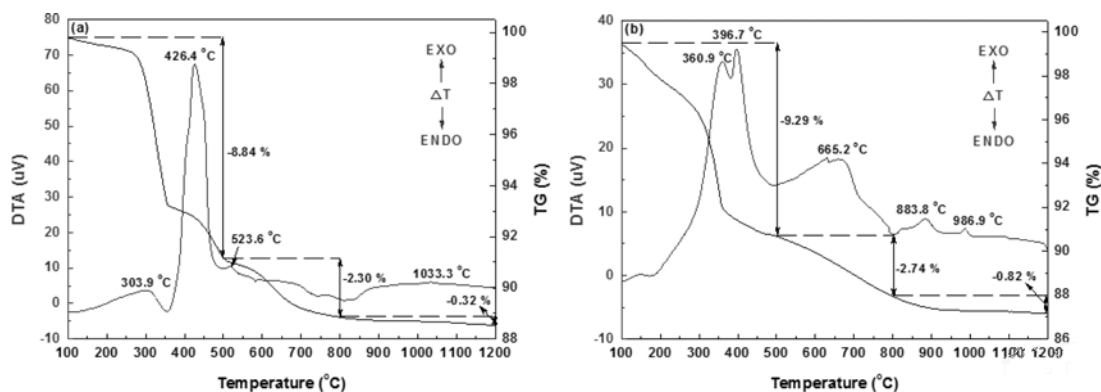


Fig. 4. The TG-DTA curves of raw material mixtures unground (a) and ground at 3 h (b).

of NdOOH was between 500 and 800 °C. The third stage shows a rather small weight loss. For the raw material mixture unground, the TG curves are similar to those of the unground mixture. However, the DTA curves have significant differences in the high temperature range, especially at 800–1200 °C. For the unground raw material mixture, the exothermic peak at 1033.3 °C is corresponding to the formation of $\text{Nd}_4\text{Si}_3\text{O}_{12}$. After 3-h grinding, the formation temperature of $\text{Nd}_4\text{Si}_3\text{O}_{12}$ decreases to 883.8 °C. The temperature for $\text{Nd}_2\text{Si}_2\text{O}_7$ formation is 986.9 °C. The results also indicate that the high-energy milling can effectively reduce the formation temperature of $\text{Nd}_2\text{Si}_2\text{O}_7$.

Fig. 5 shows the SEM micrographs of the raw material mixtures unground and ground at 3 h and heat-treated at 1200 °C. In Figs. 5(a) and 5(b), the grains of $\text{Nd}_4\text{Si}_3\text{O}_{12}$ are not obvious and its shape is irregular, which is wrapped by a large amount of glass phase. For the raw material mixture ground at 3 h and heat-treated at 1200 °C, $\text{Nd}_2\text{Si}_2\text{O}_7$ grains are more distinct and its crystallinity is higher, as shown in Figs. 5(c) and 5(d), indicating that the pre-grinding of raw material favors the promotion of the crystal growth in subsequent heat-treatment process.

In order to further reduce the synthesis temperature

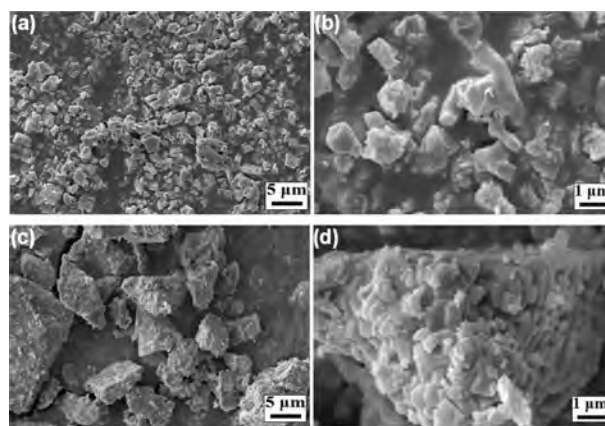


Fig. 5. The SEM images of raw material mixtures unground (a, b) and ground at 3 h (c, d) and fired at 1200 °C.

of $\text{Nd}_2\text{Si}_2\text{O}_7$ phase, different mineralizers (i.e., LiCl , H_3BO_3 and CaF_2) were added into the raw material mixtures ground at 3 h. Fig. 6 shows the XRD patterns of raw material mixtures with different mineralizers heat-treated at different temperatures, respectively. For the sample without mineralizer heat-treated at < 1000 °C, the phase is $\text{Nd}_4\text{Si}_3\text{O}_{12}$. When the sintering temperature increases to 1100 °C, $\text{Nd}_2\text{Si}_2\text{O}_7$ becomes a main crystalline

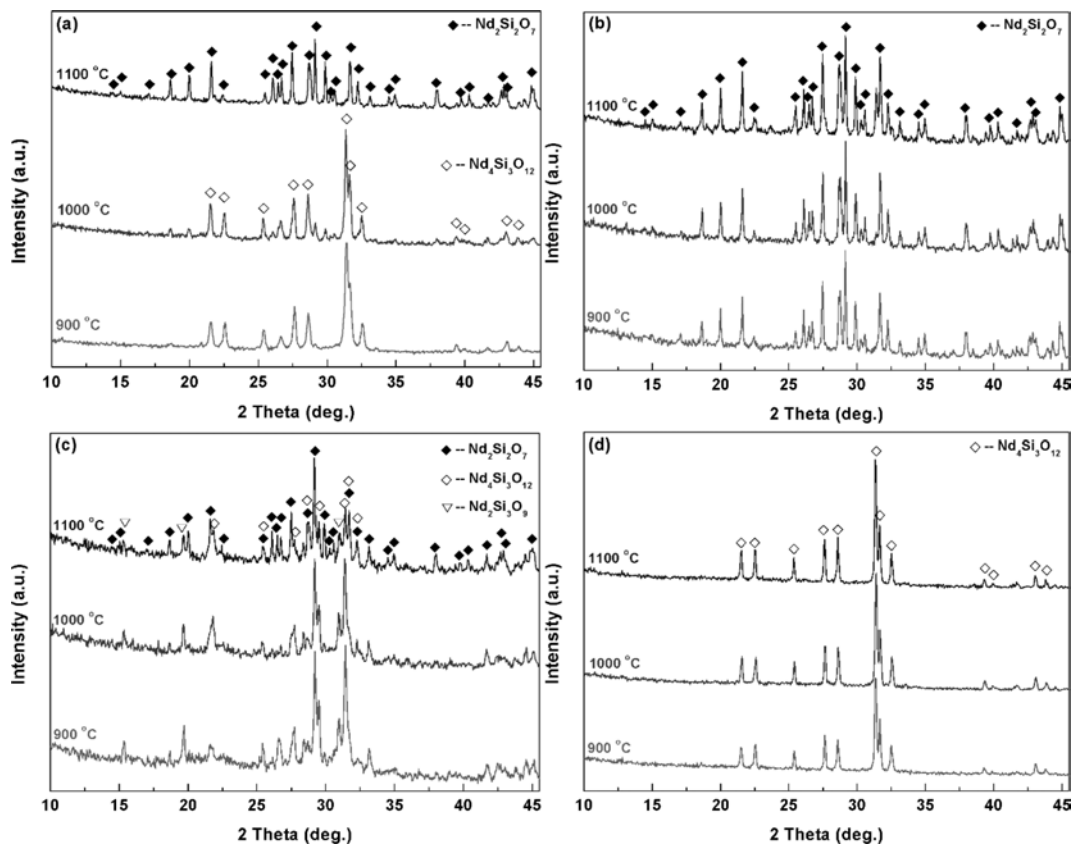


Fig. 6. The XRD patterns of samples, (a) without mineralizer, (b) with LiCl, (c) with H_3BO_3 and (d) with CaF_2 .

phase. When the mineralizer is LiCl, $\text{Nd}_2\text{Si}_2\text{O}_7$ is only crystalline phase in all the samples heat-treated at 900–1100 °C. The temperature of forming sole $\text{Nd}_2\text{Si}_2\text{O}_7$ phase is decreased by 200 °C, compared to the sample without any mineralizer. For the sample with H_3BO_3 , there are three crystal phases (i.e., $\text{Nd}_2\text{Si}_2\text{O}_7$, $\text{Nd}_4\text{Si}_3\text{O}_{12}$, and $\text{Nd}_2\text{Si}_3\text{O}_9$). The result indicates that H_3BO_3 as a mineralizer readily leads to an uneven distribution of Nd and Si components in the reaction system, which is not conducive to obtaining a single $\text{Nd}_2\text{Si}_2\text{O}_7$ phase. When the mineralizer is CaF_2 , all the samples have the single $\text{Nd}_4\text{Si}_3\text{O}_{12}$ phase, and no $\text{Nd}_2\text{Si}_2\text{O}_7$ phase appears at 900–1100 °C, indicating that the addition of fluoride changes the reaction path of the system. Fluoride and silicon oxide easily react at a high temperature (i.e., $\text{SiO}_2 + 2\text{CaF}_2 \rightarrow \text{SiF}_4\uparrow + \text{Ca}_2\text{SiO}_3$). The reaction product is silicon fluoride, which is a gaseous substance [20]. That is, the insufficient Si content leads to the formation of $\text{Nd}_4\text{Si}_3\text{O}_{12}$ phase. Therefore, the most suitable mineralizer for synthesizing $\text{Nd}_2\text{Si}_2\text{O}_7$ is LiCl.

Fig. 7 shows the DTA curves of raw material mixtures with different mineralizers. For all the samples at < 600 °C, the DTA curves are similar. However, the DTA curves have significant differences in the high temperature range. For the raw material mixture without mineralizer, the formation temperature of $\text{Nd}_4\text{Si}_3\text{O}_{12}$ is 883.8 °C and the temperature for $\text{Nd}_2\text{Si}_2\text{O}_7$ formation is

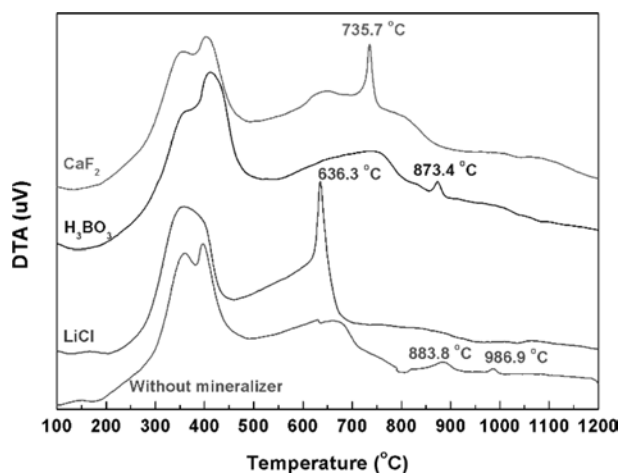


Fig. 7. The DTA curves of raw material mixtures with different mineralizers.

986.9 °C. For the DTA curve of the sample with LiCl, there is a distinct exothermic peak at 636.3 °C, which corresponds to the formation of $\text{Nd}_2\text{Si}_2\text{O}_7$. For the sample with H_3BO_3 , the formation temperature of the new phase is 873.4 °C. When the mineralizer is CaF_2 , the formation temperature of $\text{Nd}_4\text{Si}_3\text{O}_{12}$ is 735.7 °C. These results also indicate that the introduction of LiCl as a mineralizer can effectively reduce the formation

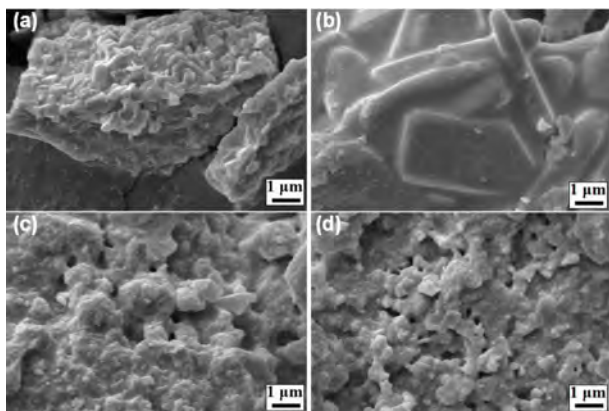


Fig. 8. The SEM images of samples with different mineralizers fired at 900 °C, (a) without mineralizer, (b) with LiCl, (c) with H_3BO_3 and (d) with CaF_2 .

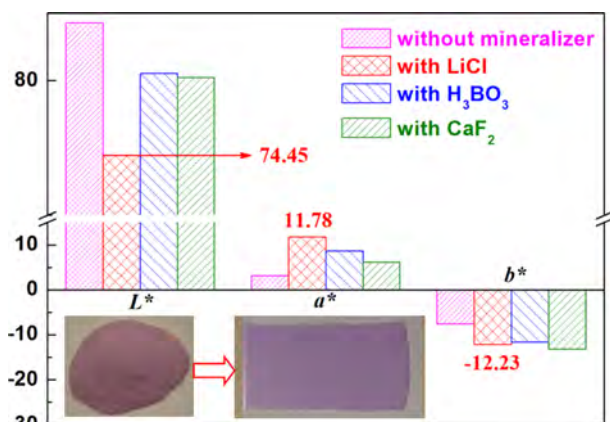


Fig. 9. L^* , a^* and b^* parameters of samples with different mineralizers fired at 900 °C.

temperature of $\text{Nd}_2\text{Si}_2\text{O}_7$.

Fig. 8 shows the SEM images of samples with different mineralizers fired at 900 °C. In Fig. 8(a), the grains are not obvious and its shape is irregular, which is wrapped by a large amount of glass phase. For the sample with LiCl (see Fig. 8(b)), there are a large number of distinct pentagonal flaky grains. The flaky grain size is approximately 4 μm and the thickness is approximately 400 nm, indicating a great crystallinity of the sample with LiCl as a mineralizer. When the mineralizer is H_3BO_3 or CaF_2 , the sample consists of agglomerates of fine particles with irregular morphology (see Figs. 8(c) and 8(d)). Therefore, the addition of LiCl as a mineralizer is also beneficial to promote the growth of $\text{Nd}_2\text{Si}_2\text{O}_7$ grain prepared by a solid-state reaction method.

Fig. 9 shows the L^* , a^* and b^* parameters of samples with different mineralizers fired at 900 °C. For a pigment powder prepared with the ground raw material mixture in the presence of LiCl as a mineralizer, the value of a^* is 11.78, and the value of b^* is -12.23, which is similar to those of the pigment powder without

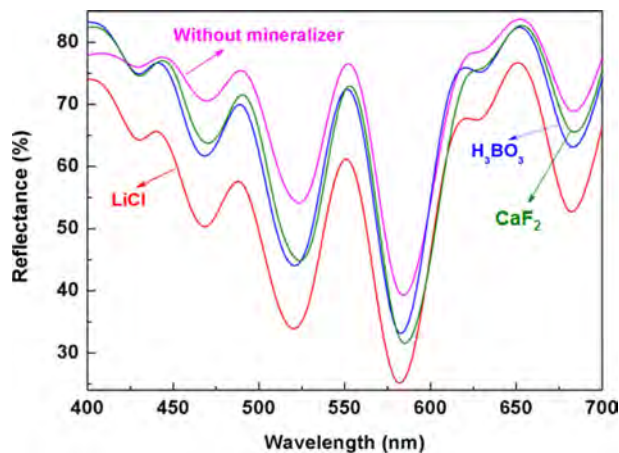


Fig. 10. The reflectance spectra of samples with different mineralizers fired at 900 °C.

mineralizer fired at 1200 °C ($a^* = 11.08$, $b^* = -13.11$). In addition, the value of a^* is close to the value of $-b^*$. This means that the pigment powder prepared with the ground raw material mixture in the presence of LiCl as a mineralizer has the equivalent degrees of red and blue hues, which can present a purple. When the mineralizer is H_3BO_3 or CaF_2 , the value of a^* is less than that of $-b^*$, implying that the pigment sample tends to blue hue. Moreover, the value of L^* for the pigment sample prepared in the presence of LiCl is the smallest, leading to a deeper color.

Fig. 10 shows the reflectance spectra of the samples with different mineralizers in the visible range from 400 nm to 700 nm. It is seen that the reflectance spectra present a high reflectivity both in low wavelength (violet and blue) and high wavelength (red) regions. Moreover, the reflectance of the sample in the presence of LiCl as a mineralizer is smaller in the visible wavelength range, leading to a deeper color. In addition, the reflectance spectra present typical Nd^{3+} absorption bands at 431, 476, 526, 582, 624 and 680 nm. All the absorption bands are assigned to the $^4\text{I}_{9/2} \rightarrow ^2\text{P}_{1/2}$, $^4\text{I}_{9/2} \rightarrow ^2\text{G}_{9/2}$, $^4\text{I}_{9/2} \rightarrow ^4\text{G}_{7/2}$, $^4\text{I}_{9/2} \rightarrow ^4\text{I}_{9/2} \rightarrow ^4\text{G}_{5/2} + ^2\text{G}_{7/2}$, $^4\text{I}_{9/2} \rightarrow ^2\text{H}_{11/2}$ and $^4\text{I}_{9/2} \rightarrow ^4\text{F}_{9/2}$ transition of Nd^{3+} ion, respectively [21]. Especially, there exist two intense absorption bands in a wavelength range of 500-600 nm (i.e., green and yellow). The reflectance spectra also exhibit a high reflectivity in low wavelength regions (i.e., violet and blue). As a result, neodymium disilicate pigment exhibits violet color under solar light.

Conclusions

$\text{Nd}_2\text{Si}_2\text{O}_7$ ceramic pigment could be synthesized via solid-phase reaction at a low temperature with pre-grinding assistance and a mineralizer (i.e., LiCl).

The raw material mixtures without pre-grinding could not form $\text{Nd}_2\text{Si}_2\text{O}_7$ phase at the sintering temperature of 1200 °C. After 3-h pre-grinding, however, sole $\text{Nd}_2\text{Si}_2\text{O}_7$

phase appeared at 1100 °C. High-energy milling process could improve the reactivity of raw materials and decrease the reaction temperature of Nd₂Si₂O₇.

Besides the decreased reaction temperature of Nd₂Si₂O₇ by pre-grinding, the temperature of forming sole Nd₂Si₂O₇ phase was further decreased by 200 °C when LiCl was used as a mineralizer. H₃BO₃ as a mineralizer readily led to an uneven distribution of Nd and Si components in the reaction system, which was not conducive to obtaining a single Nd₂Si₂O₇ phase. The sample with CaF₂ as a mineralizer could not obtain Nd₂Si₂O₇ phase. Fluoride and silicon oxide easily reacted at a higher temperature, and the insufficient Si content led to the formation of Nd₄Si₃O₁₂ phase.

In addition, the addition of LiCl as a mineralizer was beneficial to promote the growth of Nd₂Si₂O₇ grain prepared by a solid-state reaction method. Therefore, the most suitable mineralizer for solid-state synthesizing Nd₂Si₂O₇ was LiCl. The optimum synthesis temperature in the solid-state reaction was 900 °C. The Nd₂Si₂O₇ pigment exhibited violet color under solar light.

Acknowledgements

This work was supported by the China Postdoctoral Science Foundation (No. 2019M650196), the Fundamental Research Funds for the Central Universities (No. 2017 ZM013), the Major Scientific and Technological Projects of Guangdong Province (No. 2015B090927002), and the Major Scientific and Technological Projects of Foshan (No. 2016AG101415).

References

1. K.-R. Pyon, K.-S. Han, B.-H. Lee. *J. Ceram. Process. Res.* 12[3] (2011) 279-288.
2. B. Tanisan, S. Turan. *J. Ceram. Process. Res.* 12[4] (2011) 462-467.
3. Q.-K. Wang, Q.-B. Chang, Y.-Q. Wang, X. Wang, J.-E. Zhou. *Mater. Lett.* 173 (2016) 64-67.
4. Y.-Z. Halefoglu, E. Kusvuran. *J. Ceram. Process. Res.* 11[1] (2010) 92-95.
5. J.-H. Lee, H.-J. Hwang, J.-W. Kwon, J.-H. Kim, K.-T. Hwang, K.-S. Han. *J. Ceram. Process. Res.* 20[2] (2019) 127-132.
6. X.-M. He, F. Wang, H. Liu, J.-Q. Li, L.-J. Niu. *Mater. Lett.* 208 (2017) 82-85.
7. S. Jose, S.-B. Narendranath, D. Joshy, N.-V. Sajith, M.-R.-P. Kurup, P. Periyat. *Mater. Lett.* 233 (2018) 82-85.
8. S.-J. Ke, Y.-M. Wang, Z.-D. Pan. *Dyes. Pigments* 118 (2015) 145-151.
9. S.-J. Ke, Y.-M. Wang, Z.-D. Pan. *Dyes. Pigments* 108 (2014) 98-105.
10. S.-J. Ke, Z.-D. Pan, Y.-M. Wang, C.-Y. Ning, S.-L. Zheng. *Dyes. Pigments* 145 (2017) 160-167.
11. G. Brankovi, V. Vukoti, Z. Brankovi. *J. Eur. Ceram. Soc.* 27 (2007) 729-732.
12. G.-M. Min, Y. Murakami, D. Shindo. *Pow. Technol.* 104 (1999) 75-79.
13. H.-M. Yang, C.-F. Du, Y.-H. Hu. *Appl. Clay Sci.* 31 (2006) 290-297.
14. C. Gargori, S. Cerro, R. Galindo, A. Garcia, M. Llusar, G. Monros. *Ceram. Inter.* 38 (2012) 4453-4460.
15. B.-L. Lei, C. Peng, J.-Q. Wu. *J. Am. Ceram. Soc.* 95[9] (2012) 2791-2794.
16. C. Gargori, S. Cerro, N. Fas, G. Monros. *Ceram. Inter.* 43 (2017) 5490-5497.
17. H. Hamano, Y. Kuroda, Y. Yoshikawa. *Langmuir* 16 (2000) 6961-6967.
18. M. Nagao, H. Hamano, K. Hirata. *Langmuir* 19 (2003) 9201-9209.
19. W.-Q. Zhu, J. Ma, L. Xu. *Mater. Chem. Phys.* 122 (2010) 362-367.
20. R.-A. Eppler. *J. Am. Ceram. Soc.* 53 (1970) 457-462.
21. H. Onoda, K. Kojima, H. Nariai. *J. Alloys Compd.* 408 (2006) 568-572.